Integrative Biology

RSC Publishing

PAPER

View Article Online
View Journal

A high-throughput nanoimmunoassay chip applied to large-scale vaccine adjuvant screening†

Cite this: DOI: 10.1039/c3ib20263a

Jose L. Garcia-Cordero,‡[a] Chiara Nembrini,‡[a] Armando Stano,[a] Jeffrey A. Hubbell*[ab] and Sebastian J. Maerkl*[a]

Large-scale experimentation is becoming instrumental in enabling new discoveries in systems biology and personalized medicine. We developed a multiplexed high-throughput nanoimmunoassay chip capable of quantifying four biomarkers in 384 5 nL samples, for a total of 1536 assays. Our platform, compared to conventional methods, reduces volume and reagent cost by ~1000-fold. We applied our platform in the context of systems vaccinology, to assess the synergistic production of inflammatory cytokines from dendritic cells (DCs) stimulated with 10 different adjuvants that target members of the Toll-like receptor (TLR) family. We quantified these adjuvants both alone and in all pairwise combinations, for a total of 435 conditions, revealing numerous synergistic pairs. We evaluated two synergistic interactions, MPLA + Gardiquimod and MPLA + CpG-B, in a mouse model, where we measured the same inflammatory cytokines in bronchoalveolar lavage and in blood serum at 4 different time points using our chip, and observed similar synergistic effects *in vivo*, demonstrating the potential of our microfluidic platform to predict agonistic immunogenicity. More generally, a high-throughput, matrix-insensitive, low sample volume technology can play an important role in the discovery of novel therapeutics and research areas requiring large-scale biomarker quantitation.

Received 3rd November 2012,
Accepted 9th February 2013

DOI: 10.1039/c3ib20263a

www.rsc.org/ibiology

Insight, innovation, integration

Tools that facilitate large-scale biomarker quantitation at low-cost would have a significant impact in systems biology and personalized medicine. Here, we report a multiplexed microfluidic chip that performs 384 sandwich immunoassays from 5 nL volume samples, which allows for a ~1000-fold reduction in reagent cost compared to ELISA. The chip was applied to systematically study the effect of different concentrations and combinations of TLR agonists on the production of four inflammatory cytokines from dendritic cells. Out of these 405 pairwise combinations tested, two synergistic combinations, MPLA + Gardiquimod and MPLA + CpG-B, were then validated *in vivo*. This study demonstrates the potential of our screening approach to find effective adjuvant combinations and thus help in the quest to develop new vaccines.

Methods for detecting and quantitating biomolecules are fundamental tools in clinical diagnostics and life sciences. Large-scale experimentation is advancing systems biology,[1] personalized medicine,[2] and vaccinology,[3] but is still limited by the bottlenecks of classical approaches such as the enzyme-linked immunosorbent assay (ELISA) and western blotting.[1,4] While the most recent technologies, such as protein microarrays[5] or encoded microcarriers (including the Luminex system),[6–8] have drastically increased biomarker throughput, these novel immunoassays bear similar drawbacks as their classic counterparts: requirement of large sample and reagent volumes, long process and hands-on times, poor automation, excessive waste, laborious fabrication protocols in the case of microcarriers, and ultimately high costs.

The integration of microfluidics with micro/nano-scale biosensors has been touted as a solution to these technical challenges, not only by reducing sample volume and reagent consumption, but also by decreasing limits of detection (LOD), increasing throughput and multiplexing, incorporating sample pre-processing modules, and enabling automation and systems integration, while keeping the overall system simple in design and low in cost.[1,4,9,10] Assay sensitivity is important for detection of disease onset and progression.[11] As a consequence, some attention has focused on developing methods to detect

[a] Institute of Bioengineering School of Engineering and School of Life Sciences École Polytechnique Fédérale de Lausanne (EPFL), Lausanne, Switzerland. E-mail: sebastian.maerkl@epfl.ch, jeffrey.hubbell@epfl.ch
[b] Institute of Chemical Sciences and Engineering, School of Basic Sciences, École Polytechnique Fédérale de Lausanne (EPFL), Lausanne, Switzerland

† Electronic supplementary information (ESI) available. See DOI: 10.1039/c3ib20263a

‡ These authors contributed equally to this work.

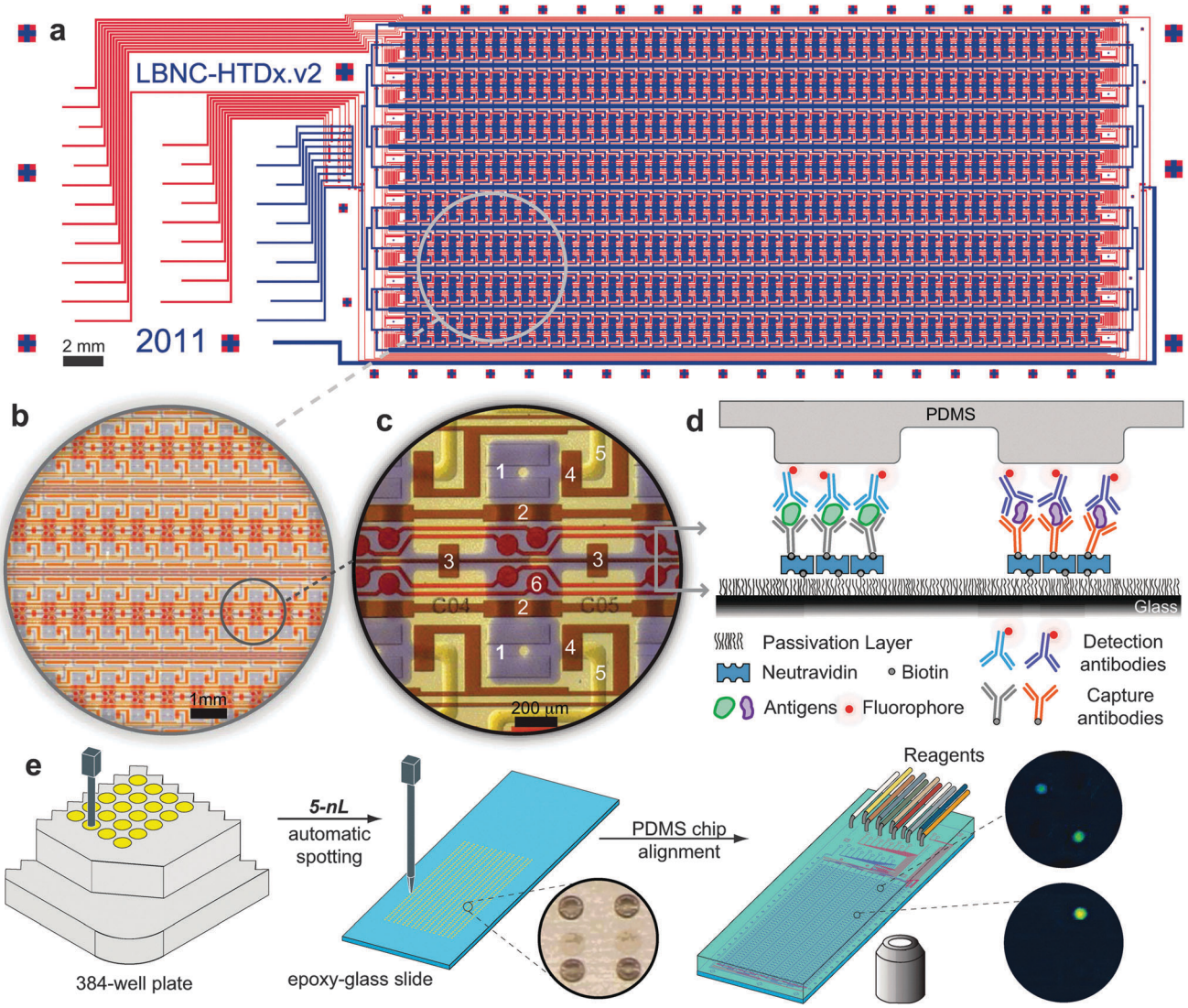

Fig. 1 Nanoimmunoassay chip workflow. The microfluidic device (a) consists of flow (blue) and control (red) layers, divided into eight rows (b), each row containing 48 single assay units for a total of 384 units. (c) Each assay unit contains two spotting chambers[1] and an assay chamber in the middle. Chamber valves[2] separate the spotting chambers from the assay chamber during surface derivatization. Assay units are isolated from one another during incubation by isolation valves.[3] Relief valves[4] help release built-up pressure into a microfluidic channel[5] after incubation. Four ''buttons'' in the assay chamber define and protect the circular immunoassay regions.[6] (d) A sandwich immunoassay is performed under each ''button'' valve with a combination of biotinylated and fluorophore-labeled antibodies. (e) Biological solutions in microtiter well-plates are automatically spotted onto an epoxy-coated glass slide using a microarray robot. Dried spots have a diameter of ~350 µm. A microfluidic chip made by multilayer soft-lithography is aligned on top of the spotted slide. Surface chemistry is generated and biomarkers are detected with a fluorescent scanner.

biomarkers at low femtomolar to attomolar concentrations.[10–13] In terms of throughput, current integrated microfluidic devices are capable of parallel detection of 12 biomarkers (multiplexing).[14] However, less progress has been made in developing automated and streamlined microsystems capable of analyzing hundreds of independent samples on a single platform from different biological matrices (throughput and matrix insensitivity). The highest throughput achieved to date on microfluidic devices is eight samples,[14,15] which need to be manually introduced, making such approaches difficult to scale and automate.[1] In this study we report a multiplexed high-throughput nanoimmunoassay chip capable of quantifying four biomarkers in 384 5 nL samples for a total of 1536 assays per device (Fig. 1a and b), which translates into a 1000-fold reduction in reagent cost (Table S1, ESI†). The limit of detection for some biomarkers is 100 fM, a similar performance to ELISA, but is achieved by detecting as few as 830 molecules in 5 nL samples (~50 zeptomoles). Here, we demonstrate the utility of our nanoimmunoassay chip to systematically study synergistic DC activation following stimulation with different Toll-like receptor (TLR) agonist combinations and doses, to guide development of novel adjuvants for vaccine formulations. Four inflammatory cytokines were simultaneously measured in cell culture medium in an *in vitro* study, as well as in serum and bronchoalveolar lavage (BAL) fluid in the *in vivo* study, demonstrating the compatibility of our assay with a number of complex biological matrices.

Materials and methods

Nanoimmunoassay chip fabrication and operation

The microfluidic device consisted of two layers. Molds for each layer were fabricated using standard lithography techniques on 4″ silicon wafers. The control and flow layer molds were patterned with the SU8 photoresist to a height of ~30 μm, and with the AZ9260 photoresist to a height of ~10 μm, respectively. Devices were cast in polydimethylsiloxane (PDMS) using the techniques of multilayer soft lithography. Microfluidic flow and control pressure regulation was achieved using a custom built pneumatic setup. Pressure for flow lines was set to 3 psi using an analog pressure gauge. Microfluidic control lines were grouped into two sets, one set for the microfluidic rounded valves and the other set for the rest of the control lines. Each set was connected to two different pressure gauges through 3-way solenoid valves. Solenoid valves were controlled from a PC by means of a graphical using interface programmed in LabView. Chip operation details are described in ESI† text.

Preparation of epoxy-silane glass slides

Our protocol for coating glass slides was adapted from Nam *et al.*[38] A solution of 720 mL of milli-Q water and ammonia solution (NH_4OH 25%) in a 5 : 1 ratio, respectively, was heated to 80 °C. Next, 150 mL of hydrogen peroxide (H_2O_2 30%) were added to the mix and glass microscope slides were bathed in the solution for 30 min. Glass slides were then rinsed with milli-Q water and dried. A solution of 1% 3-glycidoxypropyltrimethoxymethylsilane (97% pure) in toluene was prepared and the glass slides were incubated for 20 min. Glass slides were then rinsed with toluene and dried, followed by a baking step for 30 min at 120 °C. The glass slides were sonicated in toluene for 20 min, rinsed with isopropanol, and N_2 blow-dried. Glass slides were vacuum-stored at room temperature.

Automatic sample microarraying

Biological samples were pipetted into a 384-well microtiter plate. Samples were spotted in triplicate onto epoxy-silane coated glass slides using a microarray robot (QArray2) with a 4.9 nL delivery-volume spot pin (946MP8XB, Arrayit). Samples were randomly spotted on glass slides; up to three slides were spotted in one round. The humidity of the microarray robot chamber was set to 60%. A detailed protocol for spotting can be found in ESI† text.

Antibodies and recombinant cytokines

Mouse antibodies and standard proteins used were purchased from eBioscience (ESI† text). Purified primary antibodies for IL-23p19 and IL-12p35 were biotinylated using a biotinylation kit (EZ-Link Micro Sulfo-NHS-Biotinylation Kit, Thermo Fisher, USA) according to the manufacturer's instructions. All mouse secondary antibodies were conjugated with phycoerythrin (PE). We used a common secondary antibody for the detection of IL-12 and IL-23 that reacts with the p40 subunit of both cytokines.

Mice and TRL ligands

C57BL/6 mice (Charles River Laboratories) were maintained under conventional conditions in the animal facilities of EPFL. All experiments were approved by the Veterinary Authority of the Canton de Vaud, Switzerland, and were performed in accordance with Swiss legislation guidelines. Animals were between 6 and 8 weeks of age. Pam3CSK4, Pam2CSK4, polyI:C, ultrapure LPS (from *E. coli* 0111:B4), MPLA, Gardiquimod, CpG A (ODN 1585, sequence 5′-GGGGTCAACGTTGAGGGGGG-3′) and CpG C (ODN 2395, sequence 5′-TCGTCGTTTTCGGCGCGCGCCG-3′) were purchased from InvivoGen. CpG B was purchased from Microsynth (ODN 1826, sequence 5′-TCCATGACGTTCCTGACGTT-3′). Recombinant mouse EDA (extra domain A of fibronectin) was cloned in the pET-22b(+) vector and expressed in BL21DE3 *E. coli*. Chaperone proteins were removed using 2 mM ATP, and LPS contamination was removed during the purification process using 0.1% Triton X-114. Endotoxin levels were kept under 0.2 endotoxin units per microgram of protein, as tested by Limulus amebocyte assay (GenScript).

TLR agonist concentrations used in the study were chosen based on literature data as well as preliminary experiments performed in our laboratory (Table S2, ESI†). In general, 'high' concentration of an agonist induced high but not saturating levels of IL-6, TNFα and IL-12 (for a few ligands). 'Medium' concentrations were inducing lower, but still detectable cytokine levels. 'Low' concentrations were inducing little or no cytokine secretion when the ligand was administered alone (suboptimal concentration).

Bone marrow-derived dendritic cell culture

Bone marrow-derived dendritic cells (BM-DCs) were generated as previously described.[39] Briefly, bone marrow cells were flushed from the femur and tibiae of 7 week old C57BL/6 mice and cultured for 9 days in RPMI medium (Invitrogen) supplemented with 10% FBS, penicillin/streptomycin (Invitrogen), and 10 ng mL^{-1} recombinant GM-CSF (PeproTech). Fresh medium was added to the culture on day 3, 6 and 8. On day 9, cells were harvested and plated in round-bottom 96-well plates at 2×10^5 cells per well in 100 μL IMDM medium (Invitrogen) supplemented with 10% FBS and penicillin/streptomycin. Immediately after, 100 μL of IMDM medium containing the different TLR ligand mixtures were added to the cells. Medium was added to the non-activated controls. After 24 h of incubation, 160 μL supernatant were transferred to new plates and spiked with the fluorescent tracer (Alexa647-labeled dextran, 10 kDa, Invitrogen) to a 40 pM concentration. The plates were stored at −20 °C until further analysis.

ELISA validation

A pilot experiment to compare the nanoimmunoassay chip to ELISA was performed by activating BM-DCs with different concentrations of single TLR ligands. BM-DCs were activated for 24 h as described above, and the secretion of IL-6 and TNFα was measured in the supernatant by ready-set-go ELISA kits (eBioscience) or by using the nanoimmunoassay chip.

ELISA was performed according to manufacturer's instructions; plates were read on a Safire 2 microplate reader (Tecan).

In vivo TLR ligand administration

MPLA, Gardiquimod, CpG B were administered *via* the pulmonary route alone or in combination (MPLA + Gardiquimod and MPLA + CpG B) at 5 μg per mouse for each ligand. For delivery, ligands were diluted in 50 μL volume of PBS, which was then applied directly onto the mouse nostrils. Mice were bled immediately before administration (0 h), and at 6, 12 and 24 h following ligand delivery. At 24 h, mice were sacrificed and bronchoalveolar lavage was collected by cannulating and flushing the trachea 3 times with 1 mL PBS total; fluid was separated from cells by centrifugation. After the lavage, lungs were perfused with 10 mL PBS solution and digested in medium with collagenase D for 45 min, and the remaining tissue was disrupted through a cell sieve. Afterward, a 30% Percoll (VWR) gradient was applied to the cells to isolate lung leukocytes; cells were stained on the surface with fluorescently-labeled anti-CD11c, -CD11b, -MHC class II, -CD80 and -CD86 antibodies (all eBioscience) for flow cytometry analysis. A live/dead fixable dye was also included (Invitrogen). Samples were acquired on CyAn ADP Analyzer (Beckman Coulter) and data analyzed with FlowJo software (Tree Star). Lung DCs were identified by no autofluorescence, $CD11c^{high}$ and $MHC\text{-}II^{high}$ (Fig. S7, ESI†).

Results

Microarraying and microfluidics workflow

Each of the 384 assay units consists of 1.7 nL spotting chambers that encapsulate the sample (Fig. 1c). Assay units are isolated from one another during incubation steps with valves to eliminate cross-contamination. A 1 nL reaction chamber, which lies between the spotting chambers, contains four circular immunoassay regions of 60 μm in diameter created *in situ* by MITOMI "buttons".[16] Any biotinylated capture antibody can be immobilized in these regions, allowing for the parallel detection of up to four biomarkers (Fig. 1d). Samples for analysis are automatically picked from a 384-microtiter plate with a microarray robot and are arrayed on an epoxy-functionalized microscope glass slide with a 5 nL delivery-volume spotting pin (Fig. 1e). A PDMS chip is then directly aligned on top of the sample array and bonded. After derivatization of the chip surface and immobilization of the biotinylated capture antibodies in the reaction chambers, the sample spots are rehydrated and allowed to diffuse and react with the capture antibodies. A fluorescently-labeled secondary antibody is used for detecting the surface-immobilized sample molecules (Fig. 1d and e).

Chip performance

We first assessed the performance of the chip by quantifying the rehydration efficiency of the spotted samples. We spiked different concentrations of a fluorescent tracer (Alexa647-labeled dextran, 10 kDa) in undiluted serum and spotted the solutions onto the chip and rehydrated. The same solutions were flowed into the chip, and fluorescent intensity values were compared to the rehydrated values. We observed a 100% recovery of the tracer in the reaction chambers (Fig. S1a, ESI†). Spiking the fluorescent tracer into the biological samples also helps to correct for artifacts such as variability in spotted volume, viscosity, or non-specific adsorption. Samples are spiked to the same tracer concentration before spotting and the protein values measured are adjusted with the calibration curve from Fig. S1a (ESI†). Moreover, we could increase on-chip sample concentration during the spotting process by spotting the same sample multiple times on a single spot, giving rise to a three-fold higher on-chip sample concentration (Fig. S1b, ESI†). We determined the sensitivity of our platform by generating calibration curves for the cytokines IL-6, TNFα, IL-12p70 (IL-12), IL-23 in cell culture medium. We found LODs of 100 fM for IL-6 and TNFα, and 1 pM for IL-12 and IL-23 (Fig. S2, ESI†).

Comparison to ELISA

To further compare our chip to standard ELISA methods, we determined the concentration of IL-6 and TNFα in stimulated cell culture samples known to express both cytokines at a wide concentration range. Samples were analyzed on-chip in triplicates, including 8 known protein dilutions for calibration curves of each cytokine, as well as 10 negative controls, for a total of 234 samples and 428 data points. Correlation coefficients of R^2 = 0.89 and 0.9 between ELISA and on-chip results were found for IL-6 and TNFα, respectively (Fig. S3, ESI†). To evaluate the stability, reproducibility, and robustness of our platform over time, sample arrays spotted on the same day were quantitated one and five days later and similar correlations were found (Fig. S4, ESI†).

In vitro study

We applied the nanoimmunoassay platform to high-throughput screening of adjuvant combinations in order to discover synergistic adjuvant pairs that might be useful candidates to introduce in vaccines. Currently, only a few adjuvants are licensed for vaccination in humans, however, novel formulations will be required not only for the development of prophylactic vaccines against major infectious diseases, but also for therapeutics in chronic infectious diseases and cancer, as well as autoimmunity and allergy.[17,18] Pathogen-associated molecular patterns (PAMPs) such as TLR agonists potently activate dendritic cells (DCs), thereby inducing inflammatory cytokine production, which is a critical step in shaping pathogen-specific B and T cell responses.[19] Thus, there is an increasing interest in the use of TLR-based adjuvants to improve immune responses to vaccines.[20] Notably, pathogens display multiple TLR agonists, and the most successful vaccine available, the live attenuated yellow fever vaccine, activates TLR-2, -7, -8 and -9 at the same time.[21] A broad understanding of how DCs respond to TLR ligands in combination will thus help the development of improved vaccine formulations, not only for prophylactic, but also for therapeutic purposes.[22]

We analyzed cytokine secretion by bone marrow-derived DCs following activation with 10 different TLR agonists in binary combinations, at three concentrations (high, medium, low) for each ligand, for a total of 435 different assay conditions (Table S2, ESI†).

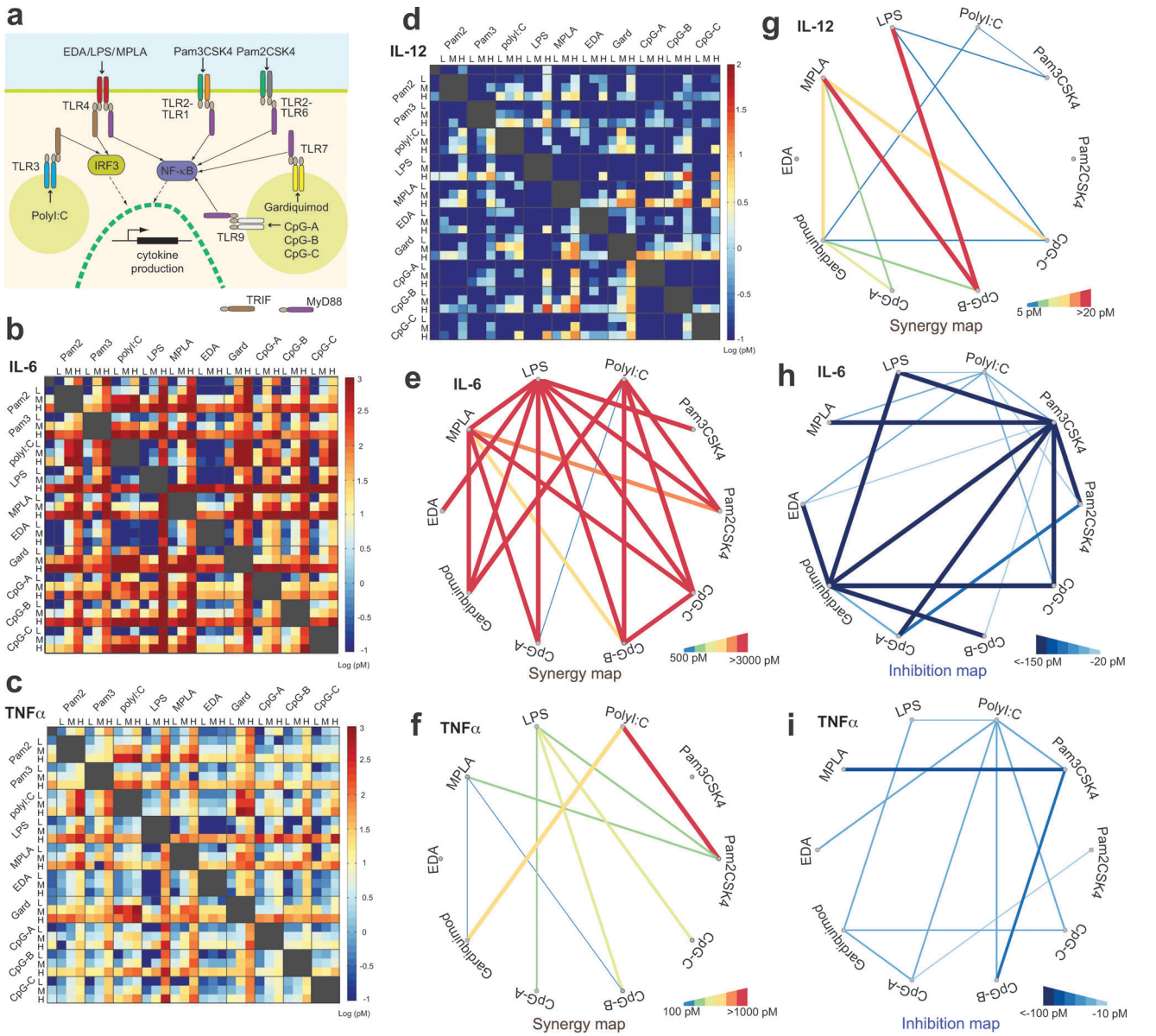

Fig. 2 Large-scale vaccine adjuvant screening results. (a) 10 different adjuvants that activate different Toll-like receptors in dendritic cells were selected for this study. All adjuvants signal through two different pathways, IRF3 and NFκB, to induce cytokine production. The TLRs may be divided into two families, ones that signal principally through the adapter molecule TRIF (among those tested, TLR-3 and TLR-4) or MyD88 (TLR-2/1, TLR-2/6, TLR-4, TLR-7 and TLR-9). (b–i) Heatmaps and synergistic and inhibitory network graphs for IL-6 (b, e, h), TNFα (c, f, i), and IL-12 (d and g). Lines connecting adjuvants in the network graphs are colored according to the difference in concentration between measured and expected values. To highlight the strongest interactions, the thickness of the lines is also proportional to the same difference. Only interactions that produced more than 5 times (synergistic) and 1/5 or less times (inhibitory) the expected additive response of combining two individual single ligands are represented in the synergistic and inhibitory map, respectively.

Agonists were chosen based on their role in boosting immune responses in preclinical or clinical studies, as well as on their capacity to activate the different TLRs and signaling pathways described in mice (Table S2, ESI† and Fig. 2a). Secretion of the inflammatory cytokines IL-6, TNFα, IL-12, and IL-23 was measured in DC culture supernatants 24 h after activation. Each supernatant was tested in triplicate, generating more than 10 000 data points acquired by a total of 7 chips (Fig. S5, ESI†). Fig. 2b–d show heatmaps that represent cytokine secretion levels following activation with different ligands. At a first glance, our data reveal that IL-6 (Fig. 2b) and TNFα (Fig. 2c) are readily secreted upon stimulation with almost all of the tested TLR agonists alone, and in binary combinations, whereas IL-12 production (Fig. 2d) seems more regulated. IL-23 secretion was negligible for almost all concentrations and ligands tested, suggesting that expression might require stronger or longer stimuli (Fig. S6, ESI†).

Notably, particular TLR agonist combinations have been shown to activate the immune system in a synergistic manner.[20,23,24] Synergy between specific TLR agonist combinations has been shown to significantly improve the potency of B cell as well as CD8 T cell responses following vaccination in different

animal models.[25–27] Therefore, the implementation of novel adjuvant formulations containing combinations of TLR agonists that at lower doses still induce strong immunity due to synergy may be crucial for more effective and less toxic vaccines. To unravel some of the most meaningful synergistic as well as inhibitory interactions between combinations of different ligands, we used network graphs to plot the ligand pairs that gave rise to at least 5-fold increased (Fig. 2e–g), or decreased (Fig. 2h and i), cytokine secretion as compared to the sum of the concentrations induced by the two ligands individually.

Our results show that 19 TLR ligand combinations induced synergistic secretion of IL-6 by DCs (Fig. 2e). In particular, strong synergy was observed between LPS, MPLA or polyI:C, when used in combination with CpGs, Gardiquimod or Pam2CSK4. Importantly, the CpGs, Gardiquimod, and Pam2CSK4 agonize TRL-9, -7 and -2/6, respectively (Fig. 2a), which exclusively use the adaptor molecule MyD88 to initiate signaling events and induce cytokine secretion, whereas LPS, MPLA (TLR-4 agonists) and polyI:C (TLR-3 agonist) initiate signaling events that are partly or completely dependent on the adaptor molecule TRIF. Our results support previous hypotheses suggesting that synergy between TLRs might be derived from the activation of both MyD88 and TRIF signaling pathways.[20,28]

Fewer and weaker synergistic events were observed for TNFα secretion by DCs (Fig. 2f) when compared to IL-6 secretion. However, the observed synergy between TLR agonists follows similar trends for both IL-6 and TNFα: the strongest effects were observed for TRIF-dependent polyI:C activation of TLR-3 in combination with MyD88-dependent TLR-7 or TLR-2/6 activation by Gardiquimod and Pam2CSK4, respectively.

As mentioned above, IL-12 was generally not secreted by DCs activated with only one TLR agonist at the concentrations tested, with the exceptions of Pam2CSK4, LPS, and Gardiquimod (Fig. 2d). Nonetheless, relevant synergistic effects were observed with different agonist combinations (12 in total), especially LPS and MPLA with CpG-B, but also CpG-A and -C, as well as between MPLA and Gardiquimod (Fig. 2g). Notably, IL-12 is a crucial cytokine for the activation of T helper 1 and cytotoxic T cell responses, and its induction is critical for novel vaccine formulations against intracellular pathogens, as well as cancer.

In addition to LPS and MPLA, we evaluated an additional TLR-4 agonist, the extra domain A of fibronectin (EDA), which, in contrast to the other ligands tested, is an endogenous protein and not a PAMP.[29] Our results suggest that, at the concentration tested, TLR-4 activation by EDA does not share the synergistic interactions that are observed for LPS or MPLA. Indeed, strong (with Gardiquimod) to mild (with polyI:C) inhibitory effects of EDA were observed instead (Fig. 2b and c, right panels).

Substantial inhibitory effects for IL-6 and TNFα secretion, but not IL-12, were observed for other TLR agonist pairs (Fig. 2h and i). In particular, significant inhibition of cytokine secretion was detected upon stimulation of DCs with TLR-1/2 agonist Pam3CSK4 in combination with nearly all other agonists tested. Interestingly, Pam3CSK4 has been shown to enhance immunity to vaccination in mice.[30] However, our results suggest a detrimental effect on cytokine secretion by this ligand when used with other PAMPs.

As mentioned above, combinations of MPLA together with CpG-B or Gardiquimod resulted in substantial synergistic DC activation. Fig. 3 highlights these effects, and additionally indicates a dose- and cytokine-dependent regulation. Accordingly, synergy in IL-6 and TNFα production was mainly observed at intermediate doses of MPLA with Gardiquimod or CpG-B (left and right panel, respectively), while at high ligand concentrations

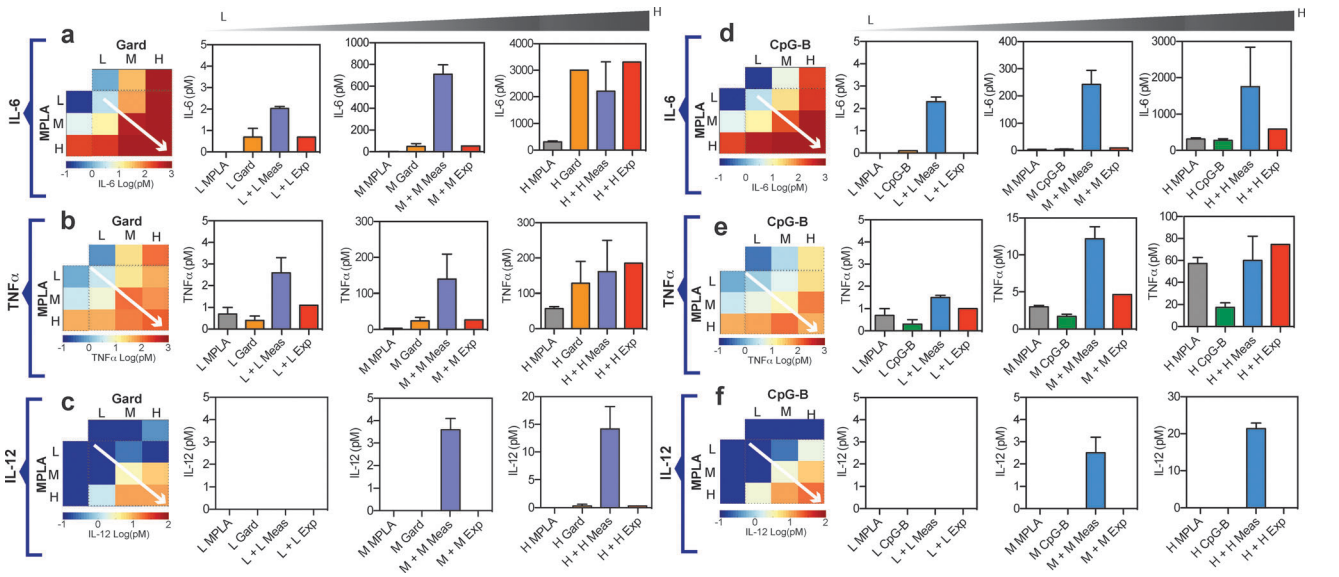

Fig. 3 Multiplexed protein measurement of *in vitro* adjuvant binary combinations. Panels show production of IL-6, TNFα and IL-12 for combinations of MPLA with Gardiquimod (a–c) and of MPLA with CpG-B (d–f). A heat map in each panel shows cytokine measurements (Meas) resulting from binary concentration combinations, in addition to individual measurements of single adjuvant stimulation. The accompanying bar graphs highlight three combinations (L + L, M + M, H + H) from the heath map (white arrow) and include a bar for the expected (Exp) additive response of the two individual ligands. Error bars, 1 s.d.

only additive and even inhibitory effects were observed, possibly indicating a saturation of signaling events following TLR activation. In contrast, IL-12 was synergistically induced when both intermediate and high agonist doses were combined (Fig. 3, bottom row). When determining the immunogenicity of different adjuvant combinations, it thus appears critical to evaluate not only combinations of cytokines but also dose responses.

In vivo study

Finally, we sought to confirm the efficacy of MPLA + Gardiquimod and MPLA + CpG-B synergistic pairs *in vivo* in mice, as well as to test the versatility of our nanoimmunoassay platform by determining cytokine concentration in biological matrices other than cell culture medium. We administered the ligands through pulmonary delivery as a route of interest for vaccines not only against airway pathogens, but also to treat other diseases such as cancer or respiratory allergy.[31] Moreover, pulmonary administration has not been evaluated previously for these ligand combinations. Cytokine secretion was determined with the nanoimmunoassay chip in mice sera at different time points and in BAL at 24 h after intranasal administration of MPLA (5 μg) ± Gardiquimod (5 μg) and MPLA (5 μg) ± CpG-B (5 μg). Up-regulation of activation markers on lung DCs was evaluated 24 h after adjuvant administration by flow cytometry.

As shown in Fig. 4a and b, CD80 and CD86 expression on lung DCs was comparable between naïve mice and mice receiving MPLA and Gardiquimod alone. In contrast, the combination of these ligands induced a significant up-regulation of CD80 expression, suggesting synergy *in vivo*. Pulmonary delivery of CpG-B alone led to lung DC activation (Fig. 4a and b), consistent with our previous measurements,[31] and addition of MPLA strengthened the effect. Systemically, a strong synergy in IL-6 serum levels was observed following administration of MPLA together with CpG-B (Fig. 4c), and IL-12 production appeared to be slightly increased by the combination (Fig. 4d). Despite the induction of DC activation, the combination of MPLA and Gardiquimod did not result in elevation of cytokines in the serum nor in the BAL. BAL IL-12 levels seemed synergistically induced by MPLA and CpG-B, however this increase was not statistically significant ($p = 0.0593$ between CpG-B and MPLA + CpG-B). Based on our *in vitro* data for these combinations we can hypothesize that a more prominent synergistic effect might be observed when testing different agonist concentration ranges.

Taken together, these data indicate the relevance of using agonist combinations for DC activation and cytokine production *in vivo*, and underline the value of our platform as a biomarker detection tool in different biological matrices.

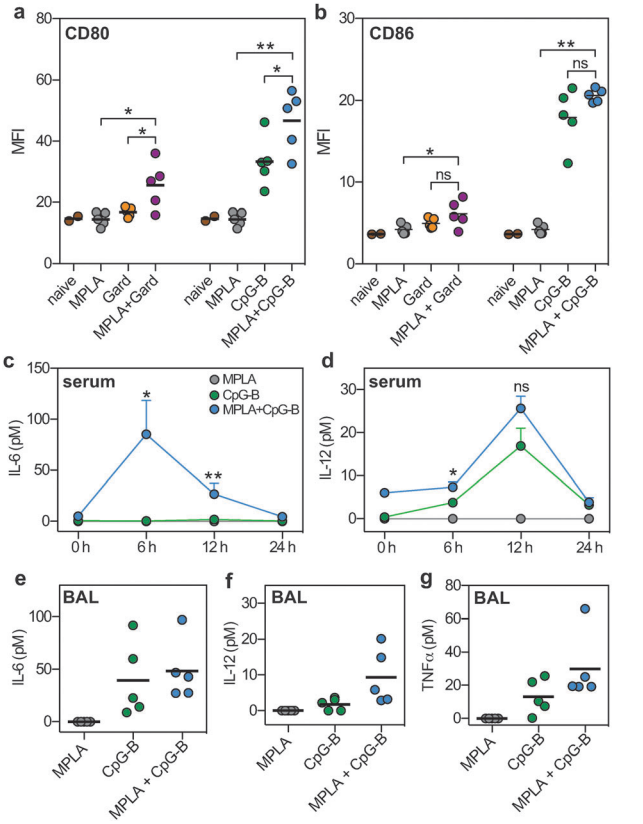

Fig. 4 Pulmonary administration of MPLA (5 μg) + Gardiquimod (5 μg) and MPLA (5 μg) + CpG-B (5 μg), as well as the agonists alone. (a and b) Lung DCs expression of the activation markers CD80 and CD86 was determined 24 h post-administration by flow cytometry and compared to levels in naïve mice. (c and d) Serum was collected at the indicated time points and IL-6 and IL-12 secretion determined with the nanoimmunoassay chip. (e–g) BAL was isolated 24 h after agonist administration and cytokine secretion determined with the microfluidic device. Results represent values from single animals or are presented as mean ± SEM. *$p < 0.05$; **$p < 0.01$: statistically significant differences as calculated by Student *t*-test; ns: not significant. Experiment was performed once with $n = 5$ mice in every group except naïve ($n = 2$).

Discussion

As large-scale studies become more prevalent in life science, including systems biology and personalized medicine, low-cost, high-throughput technologies are required to enable systematic approaches. In fact, low-cost, high-throughput instruments recently developed in the area of DNA sequencing have found applications beyond the human genome sequencing, such as the study of genetic variation, RNA expression, protein–DNA interactions and chromosome conformation.[32] Likewise, proteomic studies would benefit from similar technological advances. Here, we introduced, characterized, and applied a microfluidic technology platform for the low-cost, high-throughput quantitation of proteins in various sample matrices.

The reduction of sample volume to a few nanoliters is key to decrease the cost of reagents by at least three orders of magnitude, while delivering the same performance as the current gold standard for protein quantitation, *i.e.* ELISA. The cost of undertaking a similar study presented here would have amounted to ~€20 000 in reagent costs, whereas using our platform the cost was reduced to €15, in turn enabling larger-scale studies. Finally, low-volume sample consumption could enable kinetic biomarker quantitation in mouse sera, as well as biomarker detection in newborns, where only a few drops of blood can be drawn at a time.

The world-to-chip interface has been a major obstacle in microfluidics,[33,34] and here using a microarray robot allowed us to automatically and precisely deposit a small amount of hundreds

of samples on a surface, thus providing a simple solution to this problem. In addition, combining microfluidics with microarray technologies permits automation of the assay process and reduction of the number of required pipetting steps while increasing sample throughput by ~50-fold, as compared to currently available microfluidic platforms. The versatility of our platform is demonstrated by measuring biomarkers in different biological matrices including serum, BAL fluid, and cell culture media.

Finding effective combinations of adjuvants that act in synergy to induce potent immune responses is crucial for the rational design and development of novel vaccines.[17,20] With this large-scale study, we highlight the role of LPS and its synthetic analog MPLA in synergizing with most other TLR agonists. MPLA shares a very similar synergy profile to LPS for IL-6 and IL-12 secretion, although slightly less synergistic potency for TNFα secretion. Our results, which show a high potential for synergy, are encouraging, considering that MPLA is the only known TLR agonist used as an adjuvant in vaccines currently approved for use in humans.[20] Thus, the addition of an additional TLR ligand acting in synergy with MPLA might lead to the development of more effective vaccines. In particular, we show that DC activation by MPLA together with Gardiquimod or CpG-B gave rise to the strongest synergies *in vivo*, especially in the induction of IL-12, suggesting that such formulations may be highly promising for induction of cytotoxic T lymphocyte (CTL) responses. Combinations of MPLA and other TLR-7 and -9 agonists have only just started to be evaluated in prophylactic vaccines.[25,35] For therapeutic purposes such as in cancer, promising results have been obtained with these ligands when used alone, and their combinations might thus result in even more potent vaccines.[36]

In conclusion, the systems approach we employed here to study the effect of TLR-agonists on DCs highlights the utility of a low-cost multiplexed nanoimmunoassay chip to enable large-scale screening studies, and in this case predict immunogenicity and synergy of adjuvant combinations. We anticipate that our platform can have a significant impact not only on systems immunology and systems biology, but also more broadly on the healthcare sector. Recent reports suggest that in addition to whole genome sequencing, routine screens of biomarkers will be important to predict, treat, and prevent diseases.[2,37] Our platform is particularly suited to this challenge through the drastic cost reduction of assay cost and by enabling high-throughput, routine screening of large numbers of samples for disease indicators.

Author contributions

J.L.G.-C. and S.J.M. conceived the nanoimmunoassay chip technology, J.L.G.-C., C.N., A.S., J.A.H. and S.J.M. designed research, J.L.G.-C., C.N. and A.S. performed research and analyzed data, J.L.G.-C., C.N., J.A.H. and S.J.M. wrote the manuscript.

Acknowledgements

The authors would like to thank Marcel Geertz, members of the LBNC, Marie Ballester, Ziad Julier, Jeffrey Rice, Federico Tortelli, Alexandre deTitta, and Karen Dane for helpful discussions and technical assistance. EDA was provided by Ziad Julier and Mikaël M. Martino. This work was funded by an European Community's Seventh Framework grant FP7-ICT-248835 grant (to S.J.M.) and a grant from the Swiss National Science Foundation (to S.J.M.), the European Research Council grant Nanoimmune (to J.A.H.), the Bill and Melinda Gates Foundation (to J.A.H.), and a grant from the Swiss National Science Foundation (to J.A.H.).

References

1 D. N. Breslauer, P. J. Lee and L. P. Lee, Microfluidics-based systems biology, *Mol. Biosyst.*, 2006, **2**(2), 97–112.
2 R. Chen, *et al.*, Personal Omics Profiling Reveals Dynamic Molecular and Medical Phenotypes, *Cell*, 2012, **148**(6), 1293–1307.
3 B. Pulendran, S. Z. Li and H. I. Nakaya, Systems Vaccinology, *Immunity*, 2010, **33**(4), 516–529.
4 L. Hood, J. R. Heath, M. E. Phelps and B. Y. Lin, Systems biology and new technologies enable predictive and preventative medicine, *Science*, 2004, **306**(5696), 640–643.
5 P. Arenkov, *et al.*, Protein microchips: Use for immunoassay and enzymatic reactions, *Anal. Biochem.*, 2000, **278**(2), 123–131.
6 H. Lee, J. Kim, H. Kim, J. Kim and S. Kwon, Colour-barcoded magnetic microparticles for multiplexed bioassays, *Nat. Mater.*, 2010, **9**(9), 745–749.
7 R. Wilson, A. R. Cossins and D. G. Spiller, Encoded microcarriers for high-throughput multiplexed detection, *Angew. Chem., Int. Ed.*, 2006, **45**(37), 6104–6117.
8 D. C. Appleyard, S. C. Chapin and P. S. Doyle, Multiplexed Protein Quantification with Barcoded Hydrogel Microparticles, *Anal. Chem.*, 2011, **83**(1), 193–199.
9 G. M. Whitesides, The origins and the future of microfluidics, *Nature*, 2006, **442**(7101), 368–373.
10 J. L. Arlett, E. B. Myers and M. L. Roukes, Comparative advantages of mechanical biosensors, *Nat. Nanotechnol.*, 2011, **6**(4), 203–215.
11 D. M. Rissin, *et al.*, Single-molecule enzyme-linked immunosorbent assay detects serum proteins at subfemtomolar concentrations, *Nat. Biotechnol.*, 2010, **28**(6), 595–599.
12 J. M. Nam, C. S. Thaxton and C. A. Mirkin, Nanoparticle-based bio-bar codes for the ultrasensitive detection of proteins, *Science*, 2003, **301**(5641), 1884–1886.
13 R. S. Gaster, *et al.*, Matrix-insensitive protein assays push the limits of biosensors in medicine, *Nat. Med.*, 2009, **15**(11), 1327–1332.
14 R. Fan, *et al.*, Integrated barcode chips for rapid, multiplexed analysis of proteins in microliter quantities of blood, *Nat. Biotechnol.*, 2008, **26**(12), 1373–1378.
15 C. H. Zheng, *et al.*, High-throughput immunoassay through in-channel microfluidic patterning, *Lab Chip*, 2012, **12**(14), 2487–2490.
16 S. J. Maerkl and S. R. Quake, A systems approach to measuring the binding energy landscapes of transcription factors, *Science*, 2007, **315**(5809), 233–237.

17 M. L. Mbow, E. De Gregorio, N. M. Valiante and R. Rappuoli, New adjuvants for human vaccines, *Curr. Opin. Immunol.*, 2010, **22**(3), 411–416.
18 M. A. Swartz, S. Hirosue and J. A. Hubbell, Engineering approaches to immunotherapy, *Sci. Transl. Med.*, 2012, **4**(148), 148rv149.
19 B. Pulendran and R. Ahmed, Immunological mechanisms of vaccination, *Nat. Immunol.*, 2011, **12**(6), 509–517.
20 M. S. Duthie, H. P. Windish, C. B. Fox and S. G. Reed, Use of defined TLR ligands as adjuvants within human vaccines, *Immunol. Rev.*, 2011, **239**(1), 178–196.
21 T. Querec, *et al.*, Yellow fever vaccine YF-17D activates multiple dendritic cell subsets *via* TLR2, 7, 8, and 9 to stimulate polyvalent immunity, *J. Exp. Med.*, 2006, **203**(2), 413–424.
22 L. Buonaguro and B. Pulendran, Immunogenomics and systems biology of vaccines, *Immunol. Rev.*, 2011, **239**(1), 197–208.
23 G. Napolitani, A. Rinaldi, F. Bertoni, F. Sallusto and A. Lanzavecchia, Selected Toll-like receptor agonist combinations synergistically trigger a T helper type 1-polarizing program in dendritic cells, *Nat. Immunol.*, 2005, **6**(8), 769–776.
24 Q. Zhu, *et al.*, Toll-like receptor ligands synergize through distinct dendritic cell pathways to induce T cell responses, implications for vaccines, *Proc. Natl. Acad. Sci. U. S. A.*, 2008, **105**(42), 16260–16265.
25 S. P. Kasturi, *et al.*, Programming the magnitude and persistence of antibody responses with innate immunity, *Nature*, 2011, **470**(7335), 543–547.
26 Q. Zhu, *et al.*, Using 3 TLR ligands as a combination adjuvant induces qualitative changes in T cell responses needed for antiviral protection in mice, *J. Clin. Invest.*, 2010, **120**(2), 607–616.
27 T. Warger, *et al.*, Synergistic activation of dendritic cells by combined Toll-like receptor ligation induces superior CTL responses *in vivo*, *Blood*, 2006, **108**(2), 544–550.
28 A. Bagchi, *et al.*, MyD88-dependent and MyD88-independent pathways in synergy, priming, and tolerance between TLR agonists, *J. Immunol.*, 2007, **178**(2), 1164–1171.
29 J. J. Lasarte, *et al.*, The extra domain A from fibronectin targets antigens to TLR4-expressing cells and induces cytotoxic T cell responses *in vivo*, *J. Immunol.*, 2007, **178**(2), 748–756.
30 S. Gallorini, *et al.*, Toll-like receptor 2 dependent immunogenicity of glycoconjugate vaccines containing chemically derived zwitterionic polysaccharides, *Proc. Natl. Acad. Sci. U. S. A.*, 2009, **106**(41), 17481–17486.
31 C. Nembrini, *et al.*, Nanoparticle conjugation of antigen enhances cytotoxic T-cell responses in pulmonary vaccination, *Proc. Natl. Acad. Sci. U. S. A.*, 2011, **108**(44), E989–E997.
32 J. Shendure and H. L. Ji, Next-generation DNA sequencing, *Nat. Biotechnol.*, 2008, **26**(10), 1135–1145.
33 J. Liu, C. Hansen and S. R. Quake, Solving the ''world-to-chip'' interface problem with a microfluidic matrix, *Anal. Chem.*, 2003, **75**(18), 4718–4723.
34 C. K. Fredrickson and Z. H. Fan, Macro-to-micro interfaces for microfluidic devices, *Lab Chip*, 2004, **4**(6), 526–533.
35 V. S. Raman, *et al.*, Applying TLR synergy in immunotherapy: implications in cutaneous leishmaniasis, *J. Immunol.*, 2010, **185**(3), 1701–1710.
36 T. W. Dubensky Jr. and S. G. Reed, Adjuvants for cancer vaccines, *Semin. Immunol.*, 2010, **22**(3), 155–161.
37 R. Chen and M. Snyder, Systems biology: personalized medicine for the future?, *Curr. Opin. Pharmacol.*, 2012, **12**(5), 623–628.
38 Y. Nam, D. W. Branch and B. C. Wheeler, Epoxy-silane linking of biomolecules is simple and effective for patterning neuronal cultures, *Biosens. Bioelectron.*, 2006, **22**(5), 589–597.
39 M. B. Lutz, *et al.*, An advanced culture method for generating large quantities of highly pure dendritic cells from mouse bone marrow, *J. Immunol. Methods*, 1999, **223**(1), 77–92.